



# Modelling the thermal conductivity of a melting snow layer on a heated pavement



Anne D.W. Nuijten<sup>a,\*</sup>, Knut V. Høyland<sup>a,b</sup>

<sup>a</sup> Department of Civil and Environmental Engineering, Norwegian University of Science and Technology, Trondheim, Norway

<sup>b</sup> Sustainable Arctic Marine and Coastal Technology (SAMCoT), Centre for Research-based Innovation (CRI), Norwegian University of Science and Technology, Trondheim, Norway

## ARTICLE INFO

### Keywords:

Snow melting  
Thermal conductivity  
Compressed and uncompressed snow  
Heated pavements  
Finite difference model

## ABSTRACT

A snow layer on a heated pavement strongly affects the energy balance at the pavement surface. Freshly fallen snow has a fairly low thermal conductivity and acts as a good insulator. The thermal properties can vary greatly during the melting process. This study looks into the change of the thermal conductivity during the melting process of dry uncompressed and compressed snow on heated pavements. The energy balance of the heated pavement system is described and the effective thermal conductivity of the melting snow layer during the melting process of snow on a heated pavement system is calculated based on the volume fractions and thermal conductivity of ice, water and air. The results show that the thermal conductivity of an uncompressed and compressed melting snow layer on a heated pavement can be best described as a combination of a parallel and series system. Ice and air are modelled as a series system and water and ice/air are modelled in parallel.

## 1. Introduction

A snow layer on a heated pavement strongly affects the energy balance at the pavement surface. Freshly fallen snow has a fairly low thermal conductivity and acts as a good insulator. The thermal properties can however vary greatly during the melting process. The thermal conductivity varies mostly with the density, but also depends on the snow microstructure. The thermal conductivity of a composite material such as snow is a function of the conductivity of the different materials, their relative fractions as well as the microstructure.

The effective thermal conductivity is often described as a function of the density (Abel's, 1893; Aggarwal et al., 2009; Sturm et al., 1997; Yen, 1981). Most relationships are based on data retrieved from thermal conductivity measurements of various types of seasonal snow with densities up to  $600 \text{ kg m}^{-3}$  and for snow with a relatively low liquid water content.

Reported values of the effective thermal conductivity range from  $0.025 \text{ W m}^{-1} \text{ K}^{-1}$  to  $0.56 \text{ W m}^{-1} \text{ K}^{-1}$  for densities from 10 to  $550 \text{ kg m}^{-3}$  (Côté et al., 2012). However, a snow density of  $550 \text{ kg m}^{-3}$  can be achieved for both dry snow with a water content of zero and volume fractions of ice and air of 60% and 40% respectively as well as for snow with a high water content and volume fractions of water, ice, air and water of for example 15%, 50% and 35% respectively. These two different types of snow should have different

thermal conductivities.

The effective thermal conductivity can be modelled based on the volume fractions of ice, water and air. The ice, water and air layers can either be modelled in parallel, in series or in another configuration. Already in 1963 Schwerdtfeger described the thermal conductivity of snow as a function of the thermal conductivity of ice and air and the densities of snow and pure ice (Schwerdtfeger, 1963a). This model is based on the thermal conductivity model for bubbly ice (Schwerdtfeger, 1963b). In this model dense snow is modelled as ice containing small air bubbles (small spheres). For the thermal conductivity of light snow, air spaces are modelled as parallelepipeds. These models only include the thermal conductivity of ice and air and can therefore only be applied to dry snow. An example of a model used to calculate the thermal conductivity of snow in which the water content is included is the numerical snow cover model SNOWPACK (Lehning et al., 2002) which is based on the work of Adams and Sato (1993) in which snow is described as uniformly packed ice spheres. In SNOWPACK the thermal conductivity of the snow is described based on the temperature, the volume fractions and thermal conductivity of ice, water and air and various constants. SNOWPACK is used mostly to describe the change of seasonal snow and has not been tested yet on heated pavements.

In later developed models, the effective thermal conductivity is modelled based on the snow microstructure using 3D images of snow obtained by microtomography (Calonne et al., 2011; Kaempfer et al.,

\* Corresponding author.

E-mail address: [anne.nuijten@ntnu.no](mailto:anne.nuijten@ntnu.no) (A.D.W. Nuijten).

2005). The snow samples used by Kaempfer et al. (2005) were subjected to a constant temperature gradient. The heat flow through the snow was measured and the thermal conductivity was calculated. The study carried out by Calonne et al. (2011) considered a wider range of snow types, but the model was still limited to the conduction through ice and air.

The relative mass fractions of ice and water as well as a proper characterization of the microstructure give a good basis for determination of the thermal conductivity. So far most studies were done on dry snow. This study looks into the change in thermal conductivity during the melting process of dry uncompressed and compressed snow on heated pavements. The snow melting process on a heated pavement (Nuijten and Høyland, 2016) was analysed to gain a better understanding of this process. The energy balance is described and the effective thermal conductivity of the melting snow layer on a heated pavement system is calculated based on the volume fractions and thermal conductivity of ice, air and water. A bulk approach is used to calculate the effective thermal conductivity of the snow layer based on measurements of a melting snow layer on a heated pavement. The thermal conductivity is calculated with a parallel and a series system and compared to the results from previous studies. Additionally a combination of a parallel and series system is proposed in which ice and air are modelled as a series system and water and ice/air in parallel. The results show that the thermal conductivity of an uncompressed and compressed melting snow layer on a heated pavement can be best described with the proposed combination of a parallel and series system.

## 2. Experimental setup and method

The snow melting experiment was executed in the cold laboratories at the Norwegian University of Science and Technology in Norway. An experimental setup of a heated pavement system was built, representative for an asphalt road with a heated pavement system. On the bottom side of the 4 cm thick asphalt plate heating films were connected. On the top side, the asphalt plates were covered with a 4 mm thick binder layer to make the structure water tight (Fig. 1). To minimize heat losses insulation was placed to the side as well as under the slabs.

The temperature at the bottom and top of the asphalt plate and on top of the binder layer was measured with thermocouples, type T (No. 1 in Fig. 1). The average temperature on top of the snow layer was measured with a SI-111, a precision infrared sensor (No. 2). The air temperature and the relative humidity were measured about 5 cm above the plate with a CS215, a temperature and RH probe (No. 3). The

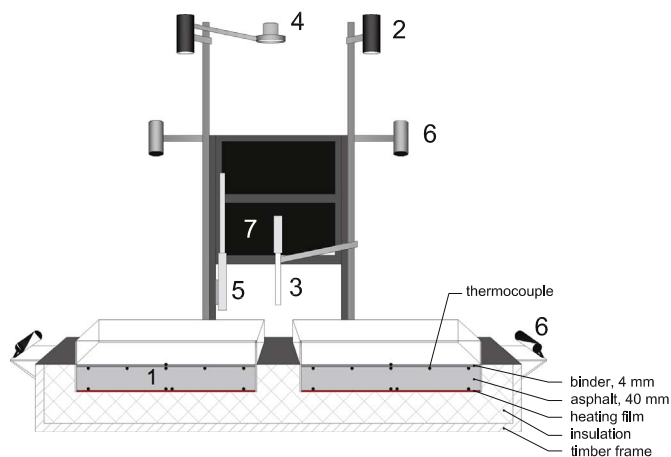


Fig. 1. Overview of the experimental setup. The setup was equipped with sensors measuring the pavement and binder temperature (No. 1), the temperature on top of the snow surface (No. 2), the air temperature and relative humidity (No. 3), the incoming longwave radiation (No. 4) and the wind speed (No. 5). On both sides as well as above the setup cameras were placed to register the change in height and surface condition (No. 6).

incoming longwave radiation was measured with a CGR3 pyrgeometer (No. 4). The wind speed was measured with a FLUKE 975 V (No. 5). Cameras were placed on the side and above the setup to register changes in the height and the surface condition (No. 6). Additionally the height was measured manually and the surface condition as observed from above was registered. The frequency of the temperature, relative humidity and longwave radiation measurements was 10 s. The frequency of the wind speed measurements was 5 min. Photos were taken every minute. The height of the snow layer was measured every 10 min with a 1 mm marked measuring stick at 9 fixed points, in a grid of  $3 \times 3$ , with distances of  $1/4$  of the width and depth of the plate between the measurement points and between the measurement points and the edges. Also every 10 min the surface condition as observed from the top was registered.

A cloudy winter night with temperatures around  $-4^\circ\text{C}$  and low wind speed was simulated. The pavement was covered with approximately 4 cm of dry snow at the start of the experiment. The snow used for this experiment was laboratory-grown snow with an average density of  $62\text{ kg m}^{-3}$ . The snow was produced with a custom-built snow machine in a cold laboratory set at  $-20^\circ\text{C}$ . For half of the tests the snow was compressed to an average density of  $150\text{ kg m}^{-3}$ . After putting the snow on the plates, the heating was switched on. The power that went into each plate was around 40 W. The power was automatically adjusted to increase the temperature of the plates to a set temperature of  $20^\circ\text{C}$ . There was a gradual increase in power during the experiment. At the start of the experiment the power was around  $350\text{--}400\text{ W m}^{-2}$  and it increased by  $50\text{--}100\text{ W m}^{-2}$  during the experiment. For a detailed description of the experimental setup and method is referred to (Nuijten and Høyland, 2016).

## 3. Thermal conductivity model

Based on the heat balance of the snow melting system the mass fluxes of ice and water and consequently the volume fractions of ice, water and air in the snow layer are calculated. The change of the snow properties is calculated based on the volume fractions.

### 3.1. Heat balance

The vertical heat balance of the snow melting system is described as:

$$q_m = q_h - q_s - q_1 - q_2 - q_3 \quad (1)$$

where  $q_m$  is the energy used to melt the snow ( $\text{W m}^{-2}$ ),  $q_h$  is the heat flux from the electric heating film underneath the asphalt ( $\text{W m}^{-2}$ ),  $q_s$  is the surface heat flux and  $q_1$ ,  $q_2$  and  $q_3$  is the heat which is absorbed by the snow layer, binder layer and asphalt layer.  $q_1$ ,  $q_2$  and  $q_3$  are given as:

$$q_n = \rho_n c_{p,n} \left( \frac{\partial T}{\partial t} \right)_n z_n \quad \text{for materials } n = 1, 2, 3 \quad (2)$$

where  $\rho$  is the density ( $\text{kg m}^{-3}$ ),  $c_p$  is the specific heat capacity ( $\text{J kg}^{-1} \text{ }^\circ\text{C}^{-1}$ ),  $\partial T/\partial t$  is the rate of temperature change ( $^\circ\text{C s}^{-1}$ ) and  $z$  is the height of the layer (m). The heat flux at the top of the snow layer  $q_s$  is given as:

$$q_s = q_{LW} + q_{conv} + q_{evap} + q_{subl} \quad (3)$$

where  $q_{LW}$  is the net longwave radiation,  $q_{conv}$  is the convective heat flux,  $q_{evap}$  is the heat flux due to evaporation and  $q_{subl}$  is the heat flux due to sublimation. An overview of the heat balance system is given in Fig. 2.

#### 3.1.1. Longwave radiation

The longwave radiative heat flux  $q_{LW}$  ( $\text{W m}^{-2}$ ) is calculated as:

$$q_{LW} = q_{LW,out} - q_{LW,in} \quad (4)$$

where  $q_{LW,out}$  is the amount of energy that the pavement surface

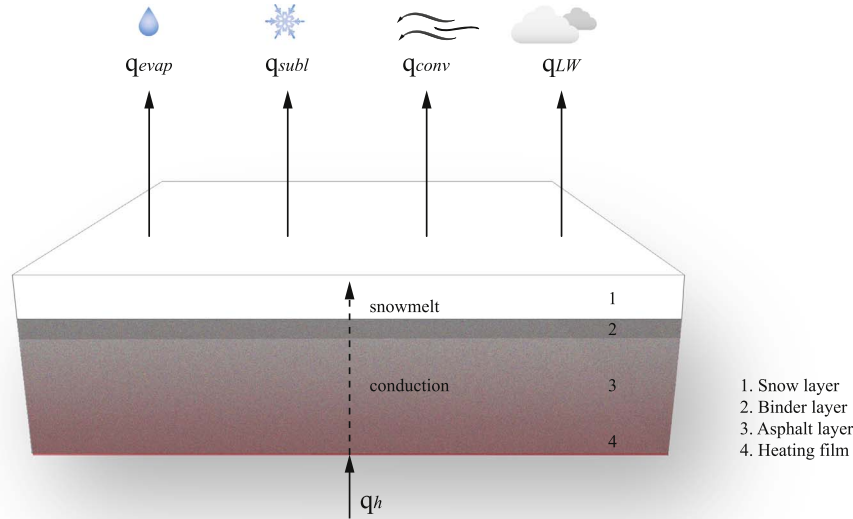


Fig. 2. Overview of the heat balance system.

radiates and  $q_{LW,in}$  the amount of incoming radiation. The incoming longwave radiation is measured. The outgoing longwave radiation is calculated as:

$$q_{LW,out} = \varepsilon_s \cdot \sigma \cdot (T_s + 273.15)^4 \quad (5)$$

where  $\varepsilon_s$  is the surface emissivity (–),  $\sigma$  is the Stephan-Boltzmann constant ( $5.68 \cdot 10^{-8} \text{ W} \cdot \text{m}^{-2} \text{ K}^{-4}$ ) and  $T_s$  is the temperature on top of the snow layer ( $^{\circ}\text{C}$ ). For  $\varepsilon_s$  a value of 0.97 is used.

### 3.1.2. Convection

The convective heat flux  $q_{conv}$  ( $\text{W m}^{-2}$ ) is given by Newton's law of cooling:

$$q_{conv} = h_c \cdot (T_s - T_a) \quad (6)$$

where  $h_c$  is the convective heat transfer coefficient (in  $\text{W m}^{-2} \text{ }^{\circ}\text{C}^{-1}$ ) and  $T_a$  is the air temperature ( $^{\circ}\text{C}$ ). Formulas for the convective heat transfer have been described by a number of authors (Bentz, 2000; Chiasson et al., 2000; Hermansson, 2004; Solaimanian and Kennedy, 1993). Dehdezi (2012) has compared the accuracy of these formulas for  $h_c$  and concluded that the formulas by Bentz (2000) and Chiasson et al. (2000) gave the best results and that the differences between those two formulas are neglectable.  $h_c$  is given as (Bentz, 2000):

$$\begin{aligned} h_c &= 5.6 + 4.0 \cdot v_w \quad \text{for } v_w \leq 5 \text{ m s}^{-1} \\ h_c &= 7.2 \cdot v_w^{0.78} \quad \text{for } v_w > 5 \text{ m s}^{-1} \end{aligned} \quad (7)$$

where  $v_w$  is the wind speed ( $\text{m s}^{-1}$ ).

### 3.1.3. Evaporation and sublimation

The heat flux for evaporation  $q_{evap/cond}$  ( $\text{W m}^{-2}$ ) and sublimation  $q_{subl/depo}$  ( $\text{W m}^{-2}$ ) are described as:

$$q_{evap/cond} = L_v \cdot \dot{m}_{wc} \quad (8)$$

$$q_{subl/depo} = L_i \cdot \dot{m}_{id} \quad (9)$$

where  $L_v$  is the latent heat of vaporization ( $\text{J kg}^{-1}$ ),  $L_i$  is the latent heat of sublimation ( $\text{J kg}^{-1}$ ),  $\dot{m}_{wc}$  is the mass flux of condensation and evaporation ( $\text{kg m}^{-2} \text{ s}^{-1}$ ) and  $\dot{m}_{id}$  is the deposition and sublimation flux ( $\text{kg m}^{-2} \text{ s}^{-1}$ ).

### 3.2. Mass fluxes

The mass flux of water  $\dot{m}_w$  ( $\text{kg m}^{-2} \text{ s}^{-1}$ ) is determined by subtracting the flux of evaporation and condensation  $\dot{m}_{wc}$  from the mass flux of

melting  $\dot{m}_m$  ( $\text{kg m}^{-2} \text{ s}^{-1}$ ):

$$\dot{m}_w = \dot{m}_m - \dot{m}_{wc} \quad (10)$$

The mass flux of ice  $\dot{m}_i$  ( $\text{kg m}^{-2} \text{ s}^{-1}$ ) is calculated as follows:

$$\dot{m}_i = -\dot{m}_m - \dot{m}_{id} \quad (11)$$

where  $\dot{m}_m$  is the mass flux of melting ( $\text{kg m}^{-2} \text{ s}^{-1}$ ) and  $\dot{m}_{id}$  is the mass flux of sublimation and deposition. A positive sign for  $\dot{m}_{wc}$  and  $\dot{m}_{id}$  indicates a positive flux from the surface to the air.  $\dot{m}_{wc}$  and  $\dot{m}_{id}$  are given by Denby et al. (2013):

$$\dot{m}_{wc} = \rho_a \cdot (\omega_s - \omega_a) / r_q \quad (12)$$

where  $\rho_a$  is the density of the air ( $\text{kg m}^{-3}$ ),  $r_q$  is the aerodynamic resistance for water vapour ( $\text{s m}^{-1}$ ) and  $\omega_a$  and  $\omega_s$  are the atmospheric and surface specific humidities, calculated based on Denby et al. (2013).  $\dot{m}_m$  is given by:

$$\dot{m}_m = \frac{q_m}{L_f} \quad (13)$$

where  $L_f$  is the latent heat of fusion and  $q_m$  is calculated according to Eq. (1).

### 3.3. Volume fractions

Based on the densities and mass fluxes of snow, water and air and the height of the snow layer the volume fractions of ice, water and air are calculated as follows:

$$1 = \theta_i + \theta_w + \theta_a \quad (14)$$

where  $\theta_i$ ,  $\theta_w$  and  $\theta_a$  are the volume fractions of ice, water and air.  $\theta_i$  and  $\theta_w$  are given as:

$$\theta_i = \frac{M_i \cdot \rho_i}{M_1 \cdot \rho_i} \quad (15)$$

$$\theta_w = \frac{M_w \cdot \rho_1}{M_1 \cdot \rho_w} \quad (16)$$

where  $M_i$ ,  $M_w$  and  $M_1$ , are the masses of ice, water and the snow layer,  $\rho_1$  is the density of the snow layer and  $\rho_i$  and  $\rho_w$  are the densities of ice and water.

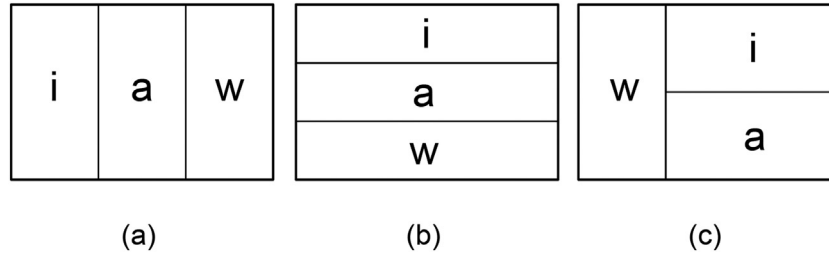


Fig. 3. Schematic overview of the parallel system (a), the series system (b) and a combination of a parallel and series system in which ice (i) and air (a) are modelled as a series system and water (w) and ice/air in parallel (c).

### 3.4. Snow properties

The specific heat capacity of the snow layer  $c_{p1}$  can be calculated as follows (Bartelt and Lehning, 2002):

$$c_{p1} = \frac{1}{\rho_1} (\rho_i \cdot c_i \cdot \theta_i + \rho_w \cdot c_w \cdot \theta_w + \rho_a \cdot c_a \cdot \theta_a) \quad (17)$$

where  $c_i$ ,  $c_w$  and  $c_a$  are the specific heat capacities of ice, water and air. The thermal conductivity of the snow layer is calculated based on the volume fractions and the thermal conductivities of ice, water and air. Three different models are being used (Fig. 3) where these are modelled as a parallel (Eq. (18)), a series (Eq. (19)), and a combination of these where the air and ice are modelled as a series system and the water and air/ice in parallel (Eq. (20)).

$$\lambda_1 = \lambda_i \cdot \theta_i + \lambda_w \cdot \theta_w + \lambda_a \cdot \theta_a \quad (18)$$

$$\lambda_1 = \frac{1}{\left(\frac{\theta_i}{\lambda_i} + \frac{\theta_w}{\lambda_w} + \frac{\theta_a}{\lambda_a}\right)} \quad (19)$$

$$\lambda_1 = \frac{\theta_i + \theta_a}{\left(\frac{\theta_i}{\lambda_i} + \frac{\theta_a}{\lambda_a}\right)} + \lambda_w \cdot \theta_w \quad (20)$$

An explicit finite difference method is used to solve the equations and to calculate the heat and mass fluxes and snow properties. At each time step, 10 s, the heat fluxes ( $q_m, t$ ) are used to calculate the mass fluxes of ice ( $\dot{m}_i, t$ ) and water ( $\dot{m}_w, t$ ). Based on these mass fluxes, the masses of ice ( $M_i, t$ ) and water ( $M_w, t$ ) are calculated. The masses of ice and water are used to calculate the volume fractions of ice ( $\theta_i, t$ ), water ( $\theta_w, t$ ) and air ( $\theta_a, t$ ) and consequently the thermal conductivity of the snow layer ( $\lambda_1, t$ ). The rate of temperature change during each time step in the different layers is calculated based on the difference between the average measured temperatures of each layer ( $(T, t + 1) - (T, t)$ ).

### 4. Input parameters

During the experiments the relative humidity fluctuated between 65% and 75% and wind speeds up to  $0.5 \text{ m s}^{-1}$  were measured (Nuijten and Høyland, 2016). Fig. 4 shows the air temperature and the temperatures in the asphalt slab and snow layer during one of the tests. As described in Nuijten and Høyland (2016) the temperatures at the bottom of the asphalt plate and 4 mm below the surface were average values at that height. At the top of the plate only one thermocouple was placed.

The temperature on top of the binder layer increased with a constant rate till it reached the melting point ( $0^\circ\text{C}$ ) after which it stayed constant for uncompressed snow and increased slightly for compressed snow. After around 130 min the surface temperature of the plate covered with compressed snow dropped to  $0^\circ\text{C}$ . At this moment the surface condition changed from wet snow into slush. Due to the stronger structure and lower permeability of the compressed snow the melt water is absorbed further into the snow without collapsing of the snow (Nuijten and Høyland, 2016). This can eventually result in air gaps between the snow and the pavement surface.

Before the temperature dropped till  $0^\circ\text{C}$  the temperatures were higher indicating that air or water was present at the pavement surface. The temperature measured on top of the snow layer reached values above  $0^\circ\text{C}$  after 120 min. While at this moment some parts of the asphalt surface were still covered with snow, at other parts all snow was melted and the meltwater was absorbed by the surrounding snow. At these open spots the temperature on top of the binder layer was measured which could rise above  $0^\circ\text{C}$ .

The density of the asphalt and binder layer is taken as  $2100 \text{ kg m}^{-3}$  (Andersland and Ladanyi, 2004) and the specific heat capacity is taken as  $0.92 \text{ kJ/kg } ^\circ\text{C}^{-1}$ .

The change in height of the uncompressed and compressed snow during the snow melting tests showed similar trends. During the first 40 min, the height of both the uncompressed and compressed snow did not change much. After an hour the height started to decrease linearly till it reached a height of 4–5 mm after which it stayed more or less constant (Nuijten and Høyland, 2016). This decrease happened when the snow changed from dry snow into slush.

At the start of the experiment the average density of the uncompressed and compressed snow was around  $60$  and  $150 \text{ kg m}^{-3}$ , respectively (Nuijten and Høyland, 2016). Fig. 5 shows the average change in density of one of the tests (continuous thin line) and the average density including the measuring error of 1 mm (dotted line). The density is calculated by dividing the weight of the snow on the plate by the volume. Towards the end of the experiment, the formula for calculating the density becomes very sensitive for small changes in the height. The height of the snow layer at the end of the experiment is 3–4 mm and the accuracy of the measuring method was around 1 mm. Since at the end of the test all snow was melted and only melt water was left the actual density was  $999.8 \text{ kg m}^{-3}$ , but this does not always correspond with the density calculated by dividing the weight of the snow by the volume. To increase the accuracy of the input data, the value at the end of the density curve is replaced with the value for the density of water ( $999.8 \text{ kg m}^{-3}$ ) and the curve is fitted for the last part of the test. The adjusted curve for one of the tests is shown as a continuous thick line in Fig. 5.

## 5. Results and sensitivity analysis

This chapter describes the change in volume fractions and the change in effective thermal conductivity during the melting process of dry uncompressed and compressed snow on a heated pavement. The results described in this chapter are the average results of six experiments performed on both uncompressed and compressed snow.

### 5.1. Volume fractions

The volume fractions are the main input parameters for the effective thermal conductivity. The accuracy of the results depends on the accuracy of the input parameters, e.g. the accuracy of the meteorological data, temperatures, the pavement properties, the height and density of the snow layer and possible heat losses near the heating film.

The heat fluxes given in Eq. (1) are integrated in time to calculate

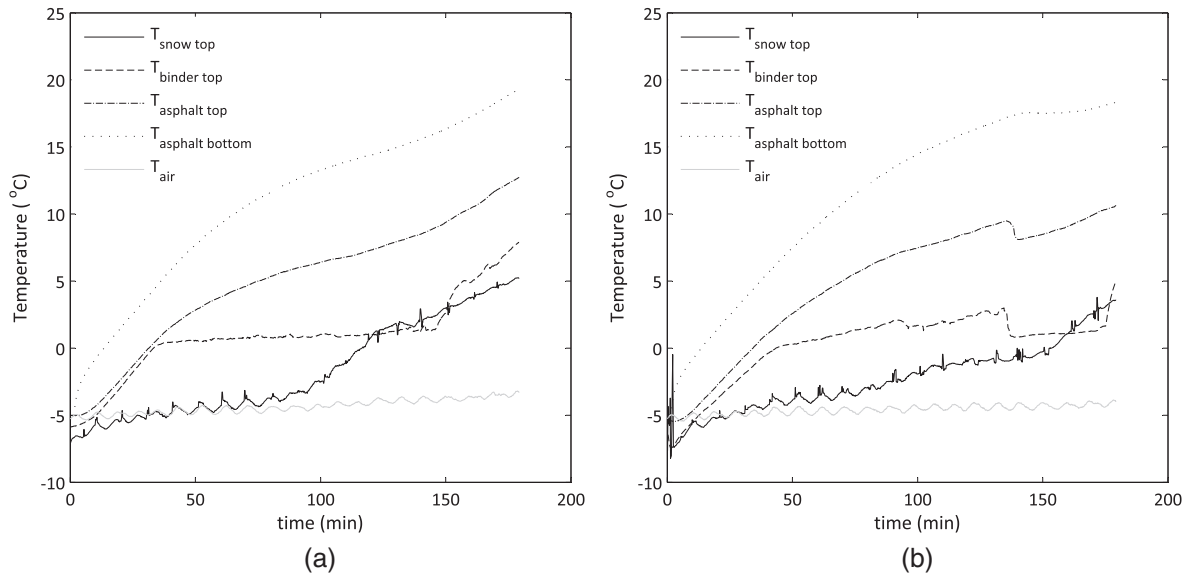


Fig. 4. Measured air temperature and temperature at the bottom and top of the asphalt plate and on top of the snow layer for (a) uncompressed and (b) compressed snow.

the heat losses during the entire experiment. Table 1 gives an overview of the average predicted total amount of energy which goes into melting, which is absorbed by the various layers and the energy which is released at the snow surface. It is assumed that the mean layer temperature is close to the bottom temperature of each layer.

It took on average 413 kJ and 418 kJ to melt all the uncompressed and compressed snow, respectively. Only 23% of the energy was used to actually melt the snow. Based on Eqs. (1) and (13) the average amount of energy to melt all snow is calculated as 100 kJ. This corresponds very well with the expected value of 100.2 kJ, which is calculated based on an average snow mass of 300 g and the latent heat of fusion (334 kJ/kg). The sum of the total amount of energy which is absorbed by the various layers and released at the snow surface is for both uncompressed and compressed snow much lower than the energy generated by the heating film. There are possibly some inaccuracies in the predicted energy that went into each layer and in the predicted energy which is released at the snow surface. There might also be additional

Table 1  
Energy balance of the heated pavement system.

	Uncompressed snow Energy [kJ]	Compressed snow Energy [kJ]
$q_s$	6	4
$q_1$	10	9
$q_2$	11	11
$q_3$	149	145
$q_m$	100	100
$q_{total}$	276	268
$q_h$	413	418

heat losses, such as for example a heat loss near the heating film, which are not included in the model.

A sensitivity study was done to look into the effect of the following parameters on the volume fractions and melting time: the height of the

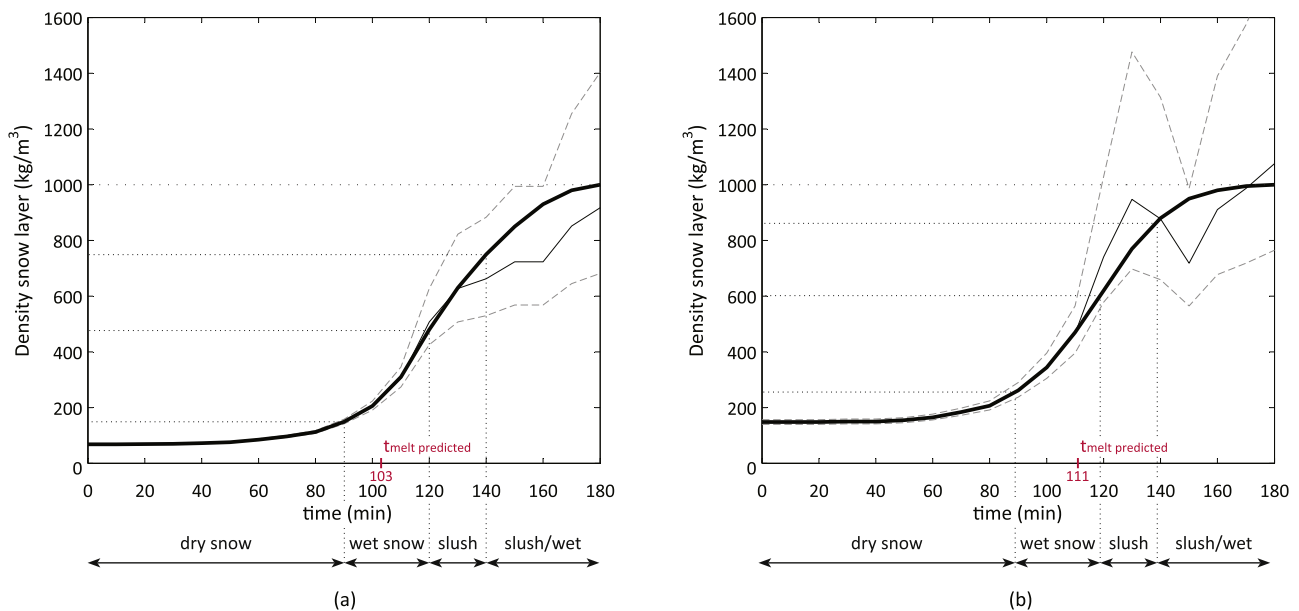


Fig. 5. Average change in density of the snow layer during one of the tests (continuous thin line), average  $\pm$  measuring error (dotted line) and an adjusted curve which ends at the density of water (continuous thick line) for uncompressed (a) and compressed snow (b). The surface conditions as observed from the top are given below the figure. The melting time as predicted by the model is shown in the figure as  $t_{melt\ predicted}$ .

**Table 2**  
Effect of the accuracy of various input parameters on the predicted average melting time of compressed and uncompressed snow.

Height snow layer			Surface flux		Pavement flux		Heating film		Assumed average layer temperature			Melting time (min)	
– 1 mm	Mean	1 mm	2.0 $q_s$	$q_s$	$q_3$	1.1 $q_3$	0.9 $q_h$	$q_h$	$T_{top}$	$T_{mean}$	$T_{bottom}$	U <sup>a</sup>	C <sup>a</sup>
	x			x	x			x		x		103	111
x				x	x			x		x		103	111
		x		x	x			x		x		103	111
	x		x		x			x		x		102	112
	x			x		x		x		x		106	115
	x			x	x		x			x		112	121
	x			x	x			x	x			98	105
	x			x	x			x			x	109	117

<sup>a</sup> Uncompressed snow (U), Compressed snow (C).

snow layer (governing the density), the surface heat flux ( $q_s$ ), the pavement heat flux ( $q_3$ ), the heat from the heating film ( $q_h$ ) and the accuracy of the calculated average temperatures in the various layers (which also affects the pavement flux). One of the input parameters of Eq. (1) is rate of temperature increase per layer. During the experiment only the top and bottom temperature of each layer (asphalt, binder, snow) were measured. In the model, a linear temperature profile per layer is assumed, while the mean temperature per layer can be closer to the top or bottom temperature of the layer.

Table 2 shows the results of the sensitivity analysis. The model originally predicts that on average the melting time is 103 and 111 min for uncompressed and compressed snow, respectively. The predicted difference in melting time between compressed and uncompressed snow corresponds well with the results of the experiment; it takes longer to melt compressed snow when the snow layers are not further physically compacted during the melting process. However, the predicted melting time of both uncompressed and compressed snow is shorter than the observed melting time (Fig. 5). The surface condition, as observed from the top consists of wet snow at the time of predicted melt, i.e. at 103 and 111 min for compressed and uncompressed snow, respectively.

The parameters affecting the volume fractions and melting time most are heat losses near the heating film, the pavement flux and the accuracy of the calculated average temperatures in the various layers. An increase in the pavement flux by 10% increases the melting time with 3 and 4 min for uncompressed and compressed snow respectively. A heat loss near the heating film of 10% increases the melting time with 9 and 10 min for uncompressed and compressed snow respectively. Assuming that the average temperature is equal to the bottom or top temperature of the layer creates a difference of 6 min compared to a linear distribution. Changing the height of the snow layer with 1 mm (the measuring error) and changing the density accordingly does not seem to have an effect on the melting time. Increasing the surface heat flux with a factor two only creates a difference in melting time of 1 min.

By including a heat loss near the heating films of 10% and assuming a mean layer temperature close to the bottom temperature of each layer, the melting time is increased to 120 and 128 min for uncompressed and compressed snow respectively, which is close to the measured transition phase from wet snow into slush (see Fig. 5).

Fig. 6 shows the change in volume fractions of ice, water and air during the melting process of uncompressed (Fig. 6a) and compressed snow (Fig. 6b). The grey and blue areas in the figure show the effect of the accuracy given in Table 2. Below the figure the predicted average surface conditions ( $P_{mean}$ ) and the surface conditions as observed from the top ( $O_{top}$ ) are given. The predicted average surface conditions are based on the volume fractions of water in snow as described in ‘The International Classification for Seasonal Snow on the Ground’ (Fierz et al., 2009). When the volume fraction is between 0 and 3% the snow is considered moist, for a volume fraction of 3–8% the snow is wet, between 8% and 15% the snow is very wet and above 15% it is soaked.

As can be seen in both figures the original model (model with the original input parameters) predicts moist and wet snow conditions long before these are observed from the top.

## 5.2. Thermal conductivity

Fig. 7 shows the change in effective thermal conductivity during the melting process of dry uncompressed and compressed snow on a heated pavement. A heat loss of 10% near the heating films is included in the figure. It is also assumed that the mean layer temperature is close to the bottom temperature of each layer. The effective thermal conductivity is calculated with a parallel system, a series system and a combined parallel/series system. The effective thermal conductivity formulas which are based on the volume fractions are compared to the formulas by Abel's (1893) - Ab, Calonne et al. (2011) - Ca, Sturm et al. (1997) - St and Yen (1981) - Ye, which were developed for snow with density values up to  $600 \text{ kg m}^{-3}$ , and with the formula by Schwerdtfeger (1963a) - Sc.

For uncompressed snow, the series and the combined parallel/series system start around the same values as the curves by Ab, Ca, St and Ye. The curves for compressed snow start at a lower value than the curves by Ab, Ca, St and Ye. For both types of snow, only the parallel system starts at a higher value. In the beginning of the test the formula by Sc gives values close to a parallel system. These values are much higher than all the other models predict.

At the end of the test, the effective thermal conductivity of the snow layer goes towards the thermal conductivity of water for the parallel, series and combined system. The formulas by Ab, Ca, St and Ye give much higher values towards the end of the test. With increasing density the formulas by Ab, Ca, Ye and Sc approach the value for the thermal conductivity of ice ( $2.1 \text{ W m}^{-1} \text{ K}^{-1}$ ). Those formulas are based on measurements on seasonal snow from a snowpack with densities up to  $600 \text{ kg m}^{-3}$  where the snow density often increases due to settling and to a lesser extent due to an increase in water content.

When dry uncompressed snow is transformed from dry into wet snow the effective thermal conductivity calculated based on the combination of the parallel and series system gives similar values compared to the formulas by Ab, Ca, St and Ye, but differs from those lines when the water content is increasing. For compressed snow a similar trend is visible, but the difference between the curves is larger.

Fig. 8 shows the effect of the accuracy of various input parameters on the accuracy of the modelled effective thermal conductivity. Height measurements have an effect on the accuracy of the modelled effective thermal conductivity, especially towards the end of the test when the snow has changed into slush. The accuracy of the calculated mean temperature per layer and the accuracy of the heat from the heating film affect the accuracy of the result for the parallel system during the first 120 min, during the change from dry snow to slush. It slightly affects the accuracy of the modelled effective thermal conductivity with the combined parallel/series system.

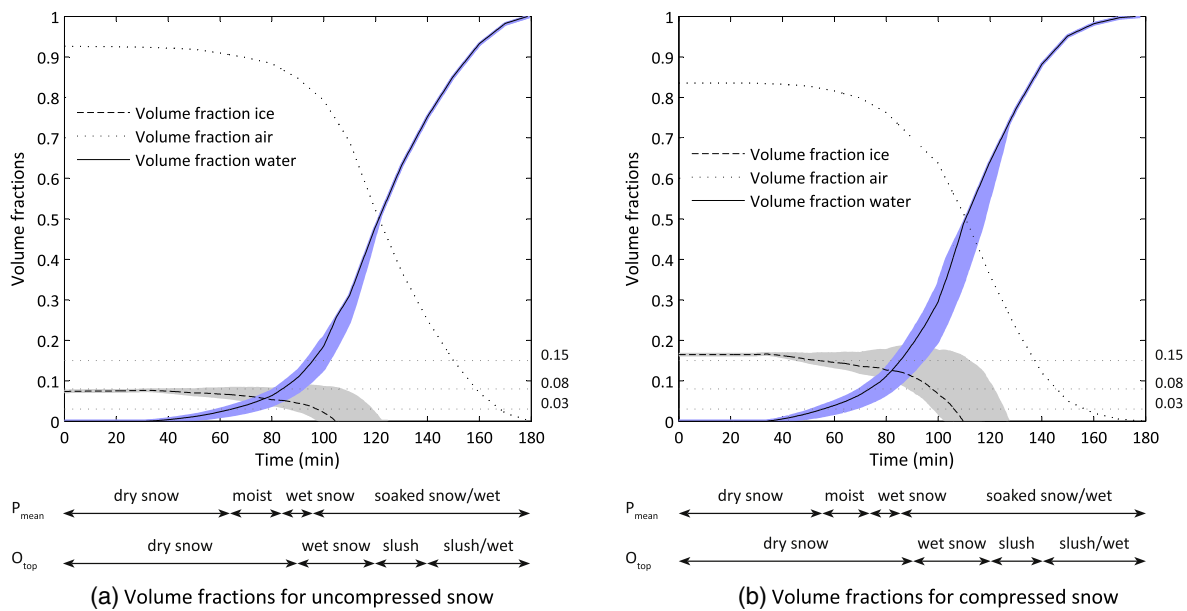


**Fig. 6.** The typical change of the volume fractions of ice, water and air during the melting process with uncompressed (a) and compressed (b) snow, based on the values used in the sensitivity analysis. The inaccuracy of the results based on the sensitivity analysis done is marked in grey (ice) and blue (water). The predicted average surface conditions ( $P_{\text{mean}}$ ) given by volume fractions predicted with the original model and as described in ‘The International Classification for Seasonal Snow on the Ground’ (Fierz et al., 2009) and the surface conditions as observed from the top ( $O_{\text{top}}$ ) are given below the figure. (For interpretation of the references to colour in this figure legend, the reader is referred to the web version of this article.)

## 6. Discussion

### 6.1. Thermal conductivity

During the first 40 min the snow had not started to melt and the surface condition consisted of dry snow and the predicted thermal conductivity of uncompressed snow based on the volume fractions should give comparable results compared to the curves by Ab, Ca, St and Ye. The series and the combined parallel/series system correspond well with these curves.

After 90–120 min wet snow was observed for both uncompressed and compressed snow. Since in the curve of Ca melt forms are included with densities up to  $600 \text{ kg m}^{-3}$  it is expected that the formulas based on the volume fractions should approach this curve for wet snow values. The parallel and a combined parallel/series correspond better to this data than the series system. The series system gives a very low thermal conductivity at the end of the test while during that period the snow has transformed into slush and thermal conductivity values around that of water are expected.

The combined system probably reflects the snow microstructure better than the parallel or series system. When snow is melted on a heated pavement the melt water is absorbed into the snow by capillary action, which can be modelled as a combination of a parallel and series system in which ice and air are modelled as a series system and water and ice/air in parallel.

### 6.2. Sensitivity analysis

The original model predicts that the uncompressed and compressed snow is melted after 120 and 128 min respectively. The model predicts a faster snow melt for both uncompressed and compressed snow than was observed during the experiment. After 120 min slush was observed from the top. The two main parameters affecting this prediction are the heating film heat flux and the pavement heat flux, which includes the temperature profile per layer. In the model no heat losses near the heating film are included, while these are expected to occur. Including these fluxes has a positive effect on the results. The pavement flux depends largely on the thermal properties of the pavement, which are estimated based on literature. Using measured properties would

improve the accuracy of the results. In addition, more accurate measurements of the temperature profile in the layer would help to improve the results.

The accuracy of the height measurements and the accuracy of the surface flux barely affect the calculated melting time. The height measurements do however affect the results of the prediction of the volume fractions and effective thermal conductivity (Fig. 8a). Towards the end of the test, when the snow layer becomes very thin, the density is more difficult to estimate based on the height measurements, as can be seen in (Fig. 5). During this last part of the test, the effect of the height measurements on the accuracy of the effective thermal conductivity prediction becomes larger.

In the model it is assumed that snow is melted once and stays melted, while in reality the water probably will refreeze after being absorbed into the snow. This process might lead to higher heat losses at the surface due to sublimation than is accounted for in the model and possibly also a longer melting time.

### 6.3. Predicted surface conditions

The original model predicts moist and wet snow conditions long before these were observed from the top (Fig. 6). This difference can partly be explained by the differences in water content within the snow layer. After 40 min the snow already started to melt at the bottom of the layer, but this was not visible from the top. The difference is also caused by the short predicted melting time by the model.

Wet and soaked snow is predicted earlier during the melting process for compressed snow than uncompressed snow, while the total snow melting takes longer for compressed snow. This difference might be explained by a difference in the snow microstructure and capillary rise between the two types of snow. The capillary rise of compressed snow is higher (Jordan et al., 1999) and water is absorbed further into the snow without collapsing of the snow.

## 7. Conclusion

A series of experiments and numerical heat balance simulations were used to estimate the effective bulk thermal conductivity of a melting snow layer. In the experiments the bottom heat flux, the

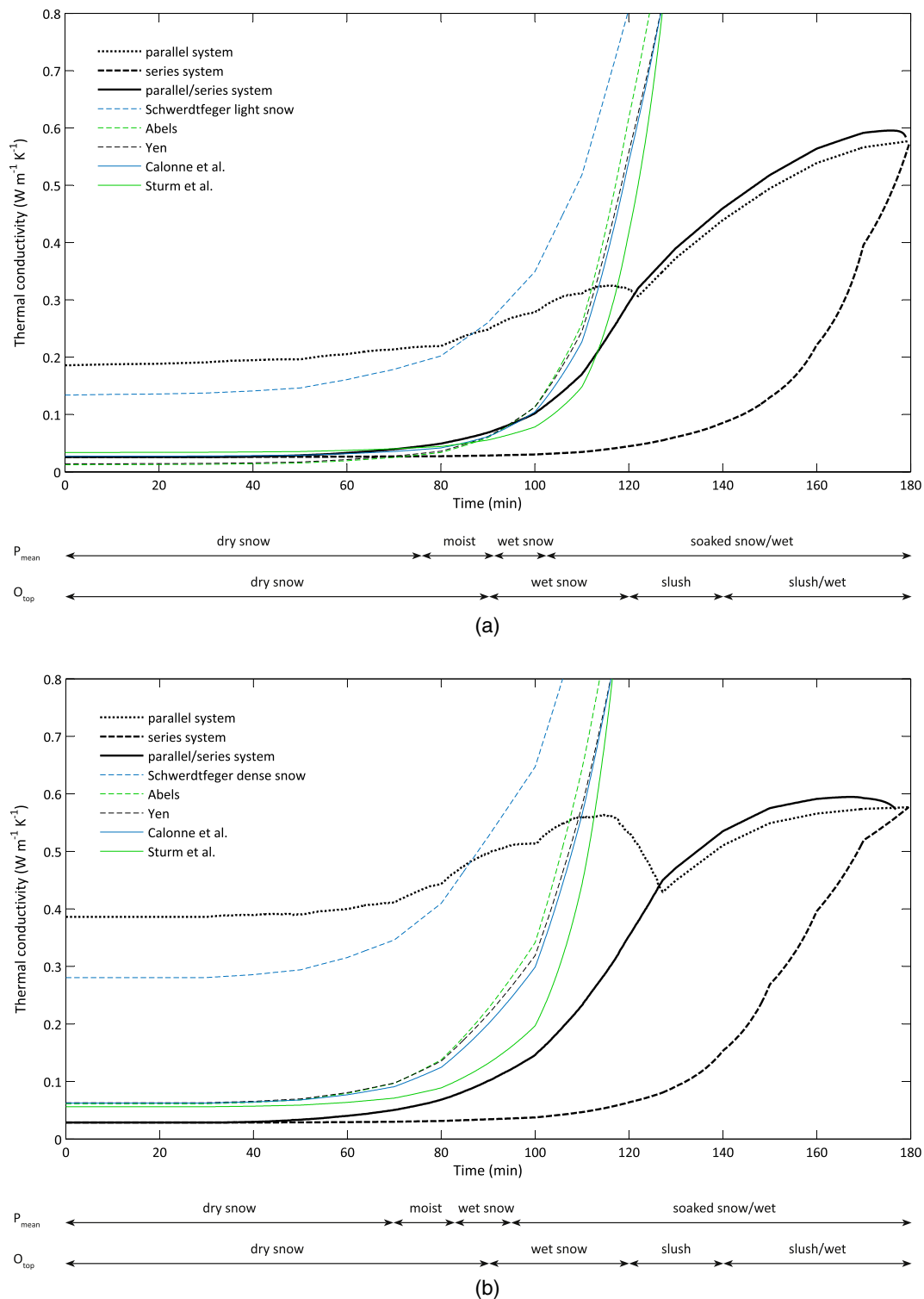
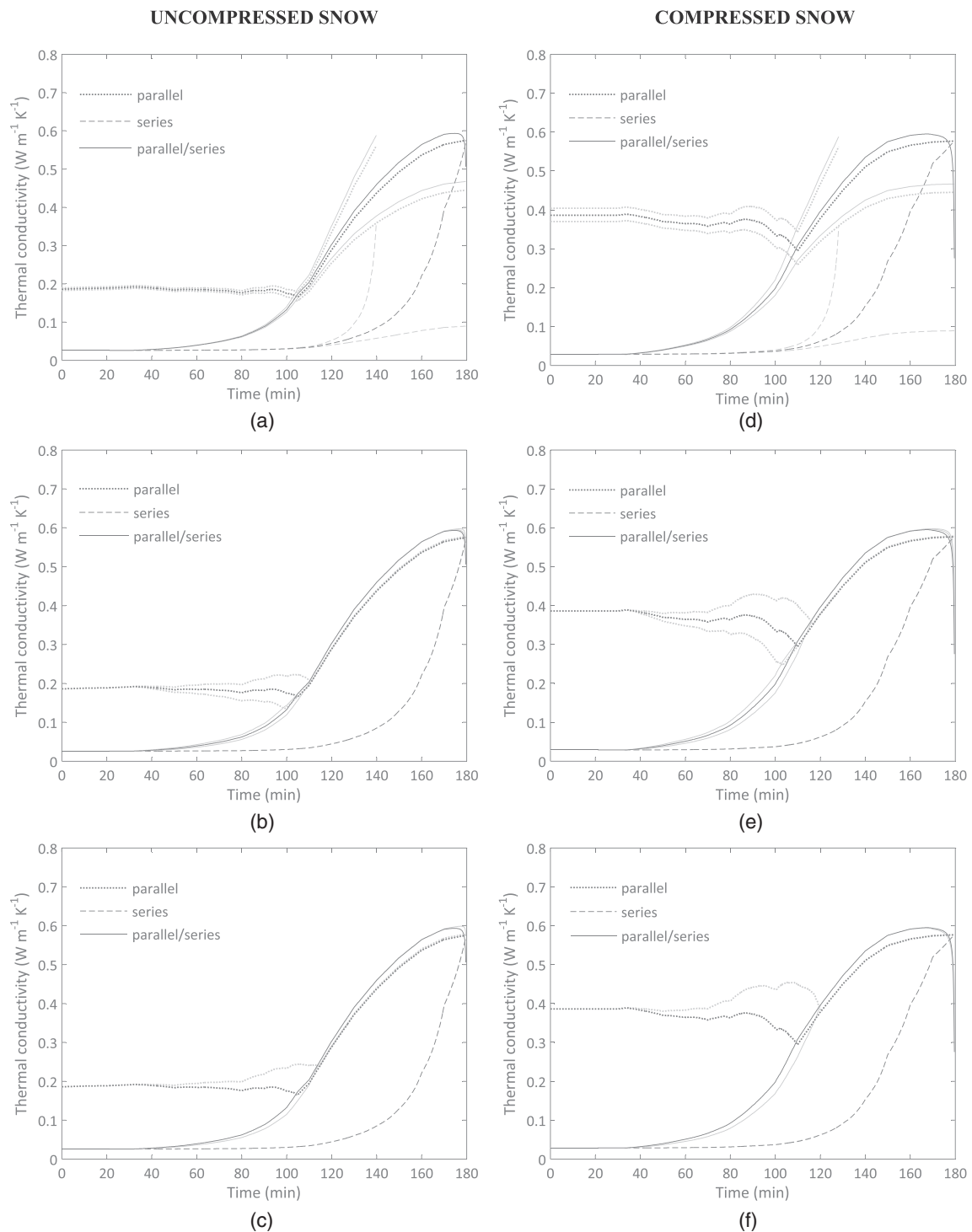


Fig. 7. Effective thermal conductivity during the melting process of dry uncompressed (a) and compressed (b) snow calculated based on the volume fractions of ice, water and air with a parallel system, a series system and a combined parallel/series system and compared to the curves by Schwedtfeger (1963a), Abels (1893), Yen (1981), Calonne et al. (2011) and Sturm et al. (1997). The surface conditions described in the figures are the surface conditions as observed from the top.

temperature profile, the snow thickness and the surface conditions were measured, and these were used as input into the numerical heat balance scheme. The mass fractions of ice, air and water and the thermal conductivity of the snow layer were calculated in time.

The bulk thermal conductivity of the snow was modelled in three simple models as a function of the mass fractions and the thermal conductivities of ice, air and water. The first model had the three

materials in series, the second in parallel and the third a series coupling of air/ice in parallel with water. In the proposed combined parallel and series system ice and air are modelled as a series system and water and ice/air are modelled in parallel. The results were compared with existing models for dry/moist snow and fitted to a final value (when all snow was melted) equal to that of water. Only the combined series/parallel fitted both the earlier (dry snow) models and resulted in the



**Fig. 8.** The effect of a) the accuracy of the height measurements, b) the accuracy of the heat flux from the heating film and c) the accuracy of the temperature profile in the pavement on the modelled effective thermal conductivity during the melting process of dry uncompressed snow, where the mean value is presented as a continuous line and the effect of the accuracy of the input parameters with dotted lines. The same plots are given for compressed snow (d–f).

value for the conductivity of water when all snow was melted. Comparing the three bulk approaches the effective thermal conductivity of a melting snow layer on a heated pavement can be best described as a combination of a parallel and series system.

The relative mass fractions of ice and water as well as a proper characterization of the microstructure give a good basis for determination of the thermal conductivity. Compared to more sophisticated models that consider the microstructure in detail this approach gives limited information about the properties of and variation within the

snow layer, but it is a more simple approach which does not need as much snow characterization.

This model is validated with measurements of a melting uncompressed and compressed snow layer. Since the proposed combined series/parallel system fitted the results from earlier models and gave a value equal to that of water when all snow was melted, it is expected that this model can be used for determining the thermal conductivity of a melting snow layer under other conditions as well, but this needs to be verified with further experiments. The results of the combined

series/parallel system fits earlier models best for uncompressed snow.

## Acknowledgements

This work has been made possible by the financial support from the Norwegian Public Roads Administration. The authors are grateful for their support. The authors would like to thank Jürg Schweizer and the anonymous reviewers for their constructive comments on the paper.

## References

- Abel's, G., 1893. Beobachtungen der Täglichen Periode der Temperatur im Schnee und Bestimmung des Wärmeleitungsvermögens des Schnees als Function Seiner Dichtigkeit (Observations of daily temperature variations in a snow cover) (in German). *Repert. Meteorol. Herausgegeben Kaiserlichen Akad. Wiss.* 16, 1–53.
- Adams, E.E., Sato, A., 1993. Model for effective thermal conductivity of a dry snow cover composed of uniform ice spheres. *Ann. Glaciol.* 18 (1), 300–304.
- Aggarwal, R.K., Negi, P.S., Satyawali, P.K., 2009. New density-based thermal conductivity equation for snow. *Def. Sci. J.* 59 (2), 126–130.
- Andersland, O.B., Ladanyi, B., 2004. *Frozen Ground Engineering*. John Wiley & Sons, Inc., New York.
- Bartelt, P., Lehning, M., 2002. A physical SNOWPACK model for the Swiss avalanche warning, part I: numerical model. *Cold Reg. Sci. Technol.* 35, 123–145. [http://dx.doi.org/10.1016/S0165-232X\(02\)00074-5](http://dx.doi.org/10.1016/S0165-232X(02)00074-5).
- Bentz, D.P., 2000. A computer model to predict the surface temperature and time-of-wetness of concrete pavements and bridge decks. In: NISTIR 6551. U.S. Department of Commerce.
- Calonne, N., Flin, F., Morin, S., Lesaffre, B., du Roscoat, S.R., Geindreau, C., 2011. Numerical and experimental investigations of the effective thermal conductivity of snow. *Geophys. Res. Lett.* 38 (23), L23501. <http://dx.doi.org/10.1029/2011GL049234>.
- Chiasson, A.D., Spitler, J.D., Rees, S.J., Smith, M.D., 2000. A model for simulating the performance of a pavement heating system as a supplemental heat rejecter with closed-loop ground-source heat pump systems. *J. Sol. Energy Eng.* 122 (4), 183–191.
- Côté, J., Rahimi, M., Konrad, J.-M., 2012. Thermal conductivity of compacted snow. In: Paper Presented at the Proceedings of the 15th International Specialty Conference on Cold Regions Engineering, Quebec City, Canada.
- Dehdezi, P.K., 2012. *Enhancing Pavements for Thermal Applications*. Department of Civil Engineering, Nottingham Transportation Engineering Centre, The University of Nottingham.
- Denby, B.R., Sundvor, I., Johansson, C., Pirjola, L., Ketzl, M., Norman, M., Kupiainen, K., Gustafsson, M., Blomqvist, G., Kauhaniemi, M., Omstedt, G., 2013. A coupled road dust and surface moisture model to predict non-exhaust road traffic induced particle emissions (NORTRIP). Part 2: surface moisture and salt impact modelling. *Atmos. Environ.* 81, 485–503. <http://dx.doi.org/10.1016/j.atmosenv.2013.09.003>.
- Fierz, C., Armstrong, R.L., Durand, Y., Etchevers, P., Greene, E., McClung, D.M., Nishimura, K., Satyawali, P.K., Sokratov, S.A., 2009. The International Classification for Seasonal Snow on the Ground (Technical Documents in Hydrology N°83, IACS Contribution N°1, UNESCO-IHP ed.), Paris.
- Hermansson, Å., 2004. Mathematical model for paved surface summer and winter temperature comparison of calculated and measured temperatures. *Cold Reg. Sci. Technol.* 40, 1–17.
- Jordan, R.E., Hardy, J.P., Perron, F.E., Fisk, D.J., 1999. Air permeability and capillary rise as measures of the pore structure of snow: an experimental and theoretical study. *Hydrol. Process.* 13 (12–13), 1733–1753. [http://dx.doi.org/10.1002/\(SICI\)1099-1085\(199909\)13:12<1733::AID-HYP863>3.0.CO;2-2](http://dx.doi.org/10.1002/(SICI)1099-1085(199909)13:12<1733::AID-HYP863>3.0.CO;2-2).
- Kaempfer, T.U., Schneebeli, M., Sokratov, S.A., 2005. A microstructural approach to model heat transfer in snow. *Geophys. Res. Lett.* 32, L21503. <http://dx.doi.org/10.1029/2005GL023873>.
- Lehning, M., Bartelt, P., Brown, B., Fierz, C., Satyawali, P., 2002. A physical SNOWPACK model for the Swiss avalanche warning, part II. Snow microstructure. *Cold Reg. Sci. Technol.* 35, 147–167. [http://dx.doi.org/10.1016/S0165-232X\(02\)00073-3](http://dx.doi.org/10.1016/S0165-232X(02)00073-3).
- Nuijten, A.D.W., Høyland, K.V., 2016. Comparison of melting processes of dry uncompressed and compressed snow on heated pavements. *Cold Reg. Sci. Technol.* 129, 69–76. <http://dx.doi.org/10.1016/j.coldregions.2016.06.010>.
- Schwerdtfeger, P., 1963a. Theoretical derivation of the thermal conductivity and diffusivity of snow. *Int. Assoc. Sci. Hydrol. Publ.* 61, 75–81.
- Schwerdtfeger, P., 1963b. The thermal properties of sea ice. *J. Glaciol.* 4, 789–807.
- Solaimanian, M., Kennedy, T.W., 1993. Predicting maximum pavement surface temperature using maximum air temperature and hourly solar radiation. In: *Transportation Research Record: Journal of the Transportation Research Board*, No. 1417. Transportation Research Board of the National Academies, Washington, D.C., pp. 1–11.
- Sturm, M., Holmgren, M., König, M., Morris, K., 1997. The thermal conductivity of seasonal snow. *J. Glaciol.* 43 (143), 26–41.
- Yen, Y.C., 1981. Review of the Thermal Properties of Snow, Ice and Sea Ice. *Cold Reg. Res. and Eng. Lab., Hanover*.